ISSN 0036-0244, Russian Journal of Physical Chemistry A, 2014, Vol. 88, No. 6, pp. 995–999. © Pleiades Publishing, Ltd., 2014.
Original Russian Text © A.E. Galashev, V.A. Polukhin, 2014, published in Zhurnal Fizicheskoi Khimii, 2014, Vol. 88, No. 6, pp. 997–1001.

PHYSICAL CHEMISTRY OF NANOCLUSTERS AND NANOMATERIALS

Computer Analysis of the Stability of Copper Films on Graphene

A. E. Galashev[a] **and V. A. Polukhin**[b]

[a] *Institute of Industrial Ecology, Ural Branch, Russian Academy of Sciences, Yekaterinburg, Russia*
[b] *Institute of Materials Science and Metallurgy, Ural Federal University, Yekaterinburg, Russia*
e-mail: galashev@ecko.uran.ru

Received July 12, 2013

Abstract—The stability of copper films of three types on graphene was studied by the molecular dynamics method. Films in the form of (111) and (100) planes and elongated (111) plane of the Cu crystal were considered. The initial arrangement of the Cu atoms relative to the carbon atoms was shown to considerably affect the thermal stability of the films. The most stable film was the one formed by placing Cu atoms in the nonadjacent hexagonal cells of graphene. The horizontal mobility of Cu atoms in this film decreased, while the vertical mobility increased as the temperature increased. The most significant stresses in this film were determined by the zigzag and chair orientations of the graphene sheet.

Keywords: graphene, copper film, stress tensor, stability.

DOI: 10.1134/S0036024414060120

INTRODUCTION

Graphene, a two-dimensional conductor with a zero gap between the conduction and valence bands, has found increasingly wide application. In the majority of theoretical and computation papers, graphene was studied as a separate material and only occasionally as a material affected by a stable support of another material (Ni, Cu, SiO_2, etc.). The behavior of thin metal films on graphene was studied in few works [1]. These studies are important, e.g., in connection with the recently suggested use of graphene for preparing ink for jet printers [2].

As is known, graphene (both one- and multilayer) has high conductivity [3] and can be used as an excellent electrode [4, 5]. A shell of multilayer graphene can play a dual role of protector against oxidation for the metal nanonucleus [6–8] and a well-conducting compound with the adjacent metal nanonucleus [9]. The Cu nanoparticles covered with multilayer graphene are ideal material for preparing ink [10]. This is one of the few advantages of multilayer graphene over one-layer graphene. One-layer graphene that contacts the metal is mostly preferable because of being much more useful. For example, studies of the interaction between silver and graphene by surface-enhanced Raman scattering (SERS) showed that SERS enhancement and the degree of splitting of G branches decreased as the number of Ag-coated graphene layers increased [11]. The deposition of Ag on graphene shows itself as *n*-doping, whereas the Au film on graphene creates *p*-doping.

This opens up ample opportunities for electronics based on graphene-containing composites. Coating with one-layer graphene can offer reliable protection from corrosion when a thin coating is needed, as, e.g., for microelectronic components.

The goal of this work was to investigate the thermal stability of multilayer copper films on graphene, determine the temperature changes of stresses in them, and study the behavior of the mobility of metal atoms during their heating.

COMPUTER MODEL

The calculations were performed by the classical molecular dynamics (MD) method. Empirical potentials of three types were used: the potentials that describe carbon–carbon (in graphene), copper–copper, and copper–carbon interactions. The Tersoff potential was taken as the basis for representing interactions in graphene [12, 13]:

$$U^{\mathrm{Ter}} = \frac{1}{2}\sum_{i}\sum_{j\neq i} f_c(r_{ij})\left\{f_R(r_{ij}) + b_{ij}f_A(r_{ij})\right\},$$

$$f_R(r) = A\exp(-\lambda_1 r),$$

$$f_c(r) = \begin{cases} 1, & r < R, \\ \dfrac{1}{2} + \dfrac{1}{2}\cos\dfrac{\pi(r-R)}{S-R}, & R < r < S, \\ 0 & r > S, \end{cases} \tag{1}$$

$$f_A(r) = -B\exp(-\lambda_2 r),$$

$$b_{ij} = \left(1 + \beta^n \varsigma_{ij}^n\right), \quad \varsigma_{ij} = \sum_{k\neq i,j} f_c(r_{ik})g(\theta_{ijk}),$$

$$g(\theta) = 1 + \frac{c^2}{d^2} - \frac{c^2}{d^2 + (h - \cos\theta)^2}.$$

Here, the indices i, j, and k are the carbon atoms, r_{ij} is the length of the i–j bond, and θ_{ijk} is the angle between the i–j and j–k bonds. The parameters of (1) except S were taken from [13].

A transition to the modeling of two-dimensional systems (e.g., graphene) with a covalent bond requires modification of this potential [14]. In this model, the maximum coverage (S) of the covalent interaction was increased from 0.21 to 0.23 nm. Outside the region of covalent interaction there was the region of very weak Lennard-Jones interaction whose parameters were given in [14] and which has the character of attraction. To prevent the rotation of the graphene sheet, "deceleration" with a strength $-dV_{ij}(\Omega_{kijl})/dr_{ij}$ (the torsion potential $V_{ij}(\Omega_{kijl})$ was determined in [14]) at each atomic unit of graphene was used. The interaction between the Cu atoms was specified by the Sutton–Chen many-body potential [15]

$$U^{SC} = \varepsilon\left[\frac{1}{2}\sum_i\sum_{j\neq i}V(r_{ij}) - c\sum_i\sqrt{\rho_i}\right],$$

where

$$V(r_{ij}) = (a/r_{ij})^n, \quad \rho_i = \sum_{j\neq i}(a/r_{ij})^m.$$

The parameters of the U^{SC} potential (ε, a, c, m, and n) were given in [15].

The interaction of the C and Cu atoms was described by the Lennard-Jones potential with parameters from [16]; due to more rigid repulsion, this potential does not give the nonphysical deep mutual penetration of C and Cu atoms in contrast to the Morse potential with the parameters selected by the density functional theory method [17].

The self-diffusion coefficient was determined in terms of the mean square of the displacement of Cu atoms:

$$D = \lim_{t\to\infty}\frac{1}{2\Gamma}\left\langle[\Delta\mathbf{r}(t)]^2\right\rangle,$$

where Γ is the dimensionality of space.

The stress at the site of the i atom of the metal film was determined as [15]

$$\sigma_{\alpha\beta}(i) = \frac{\varepsilon}{2a^2\Omega_i}\sum_{i\neq j}^{k}\Big[-n(a/r_{ij})^{n+2} + mc(1/\sqrt{\rho_i} + 1/\sqrt{\rho_j})(a/r_{ij})^{m+2}\Big]r_{ij}^{\alpha}r_{ij}^{\beta},$$

where ε is the parameter with the dimensionality of energy; c is the dimensionless parameter; $\rho_i = \sum_{j\neq i}(a/r_{ij})^m$, a is the parameter with the dimensionality of length usually set equal to the lattice constant; m and n are positive integers such that $n > m$; and Ω_i is the volume of the individual atom, which may be associated with the volume of the Voronoi polyhedron linked to the i atom.

The stability of the three types of copper films on graphene having dimensions 3.4 × 4.0 nm and 406 C atoms was studied. The first copper film was the (111) plane of the fcc copper crystal and was formed of 208 Cu atoms. The film was initially placed in the middle of a graphene sheet at equal small (of the order of the diameter of the Cu atom) distances from the opposite edges of the sheet. The structure of the second film corresponded to the (100) plane of the copper crystal and had only 49 atoms. It was also placed in the middle of the graphene sheet. Its size was chosen such that the number of metal atoms corresponded to the number of Cu atoms in the third film (49 at maximum). The arrangement of Cu atoms in the first two films was not correlated with the structure of graphene. The initial arrangement of Cu atoms in the third film was a monolayer in the form of a loose (111) plane of the fcc lattice (parallel to the graphene plane) with the distance between the nearest atoms $r_{\text{Cu–Cu}} = 0.6507$ nm. The Cu atoms were right opposite to the centers of the nonadjacent hexagonal cells formed by the carbon atoms; the shortest distance between the C and Cu atoms $r_{\text{C–Cu}} = 0.2243$ nm corresponded to $r_{\text{C–Cu}}$ calculated in terms of the density functional theory [18]. In a bulk copper crystal, $r_{\text{Cu–Cu}} = 0.2556$ nm. Consequently, the Cu film was initially stretched because of the incompatibility of the lattice constants of graphene and copper. The shortest distance between the C atoms in graphene was $r_{\text{C–C}} = 0.142$ nm. The equations of motion were integrated by the fourth order Runge–Kutta method with a time step of $\Delta t = 0.2$ fs. The calculation time was $10^6\Delta t$ or 200 ps for each temperature. The calculations were started at 300 K. After each million of time steps, the temperature of the system was raised by 500 K and the next calculation was performed with the same duration. The last calculation corresponded to the temperature 3300 K. The temperature in the model was maintained with a Berendsen thermostat [19].

RESULTS AND DISCUSSION

The total energy of free single-sheet graphene calculated at $T = 300$ K is –7.02 eV, which agrees with the data of quantum-mechanical calculations (–6.98 eV) [20]. The close-packed copper monolayer was placed on the surface of graphene in such a way that none of the atoms characterized by the size $\sigma_{\text{Cu}} = 0.2277$ nm [21] (σ_{Cu} is the Lennard-Jones parameter) went beyond the limits of the graphene sheet. The arbitrary arrangement of the copper film relative to the carbon atoms was justified by the fact that the lattice constants of the metal film and graphene were incompatible. As a result, the coordinates of the centers of all 208 Cu atoms that formed the (111) plane were within the area of the graphene sheet containing 406 C atoms. However, the Cu (111) plane that was stable in a bulk copper crystal and had the shortest interatomic distance of 0.256 nm proved unstable when placed on the

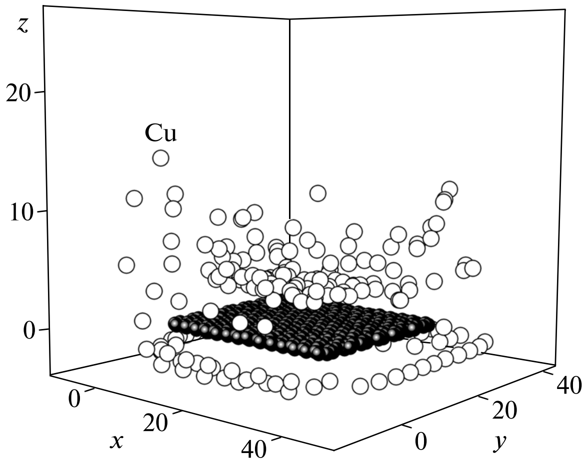

Fig. 1. Configuration of the system of a copper film on graphene, where the film is a close-packed (111) plane of Cu crystal at a moment of time of 200 ps. The atomic coordinates are given in Å.

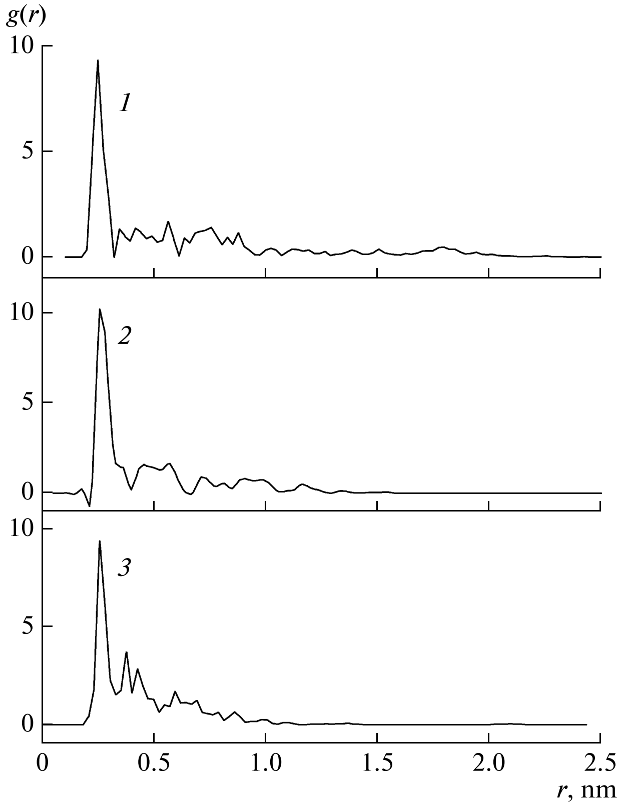

Fig. 2. Radial distribution functions (calculated for the central atom) of various Cu films on graphene: (*1*) close-packed (111) plane of copper, (*2*) (100) plane of copper, and (*3*) elongated (111) plane of copper, whose atoms occupy nonadjacent cells of the graphene lattice.

graphene sheet. The atoms of this plane initially started to move in horizontal directions parallel to the graphene plane, due to which the Cu (111) plane expanded. The terminal Cu atoms that went beyond the limits of the graphene plane lost support from graphene and abandoned the sheet (Fig. 1). By the moment of time of 200 ps, the Cu atoms lying over graphene did not form a regular packing any longer. The majority of these atoms rose over the graphene sheet and only an insignificant number of them remained in the plane parallel to the graphene sheet. The close-packed copper film thus proved unstable on the graphene sheet already at 300 K.

The arrangement of the 49 Cu atoms of the (100) face of the copper crystal in the central part of the graphene sheet did not lead to deviation of the metal atoms from the sheet by the moment of time of 200 ps. However, the nearly horizontal metal film was no longer the (100) face of the copper crystal; it had a loose structure, which was more likely to be disordered. The film proved unstable against heating; nearly half of all Cu atoms quit it already at 1800 K. Thus the lack of coordination between the packing of Cu atoms in the film and the graphene structure led to instability of the film; i.e., the effect of graphene on the state of the metal film was rather significant. The energy of the copper–graphene interaction $E_{\text{Cu–C}}$ for this film at $T = 300$ K was 22.2% of the energy of the copper–copper interaction $E_{\text{Cu–Cu}}$ (–0.28 eV, while the starting energy was $E_{\text{Cu–Cu}}^{\text{init}} = -2.4$ eV); for the first film, it was 0.3% of the corresponding $E_{\text{Cu–Cu}}$ (–2.8 eV).

The structure of the Cu film formed from 49 atoms initially placed opposite to the centers of the nonadjacent honeycombs of the 406-atomic graphene sheet was also loose, but slightly less planar. By the moment of time of 200 ps at 300 K, the Cu atoms assembled into three similarly orientated serpentine lines in the middle part of the graphene sheet. At 3300 K, the Cu atoms formed an elongated dense drop whose acute apex was "closed" by a serpentine line of 10 atoms. By the moment of time of 200 ps at this temperature, six atoms in the metal film rose above the other atoms to a distance of the order of the distance from the drop to graphene. At 300 K, the energy $E_{\text{Cu–C}}$ was 3.3% of the energy $E_{\text{Cu–Cu}}$ (–1.96 eV) for this film. The Cu film formed in accordance with the graphene structure thus showed the highest thermal stability among the films under study.

The radial distribution functions $g(r)$ of the three above-described types of the copper film on graphene are presented in Fig. 2. All these functions have a high first peak. It reflects the presence of short-range ordering in the films or, more exactly, shows that the Cu atoms in the films tend to lie at approximately the same shortest distance from one another. This distance agrees, with a good accuracy, with the distance between the nearest neighbors in the copper crystal. The other peaks of the $g(r)$ function reflect the structure with medium-range ordering. In other words, they show how the neighbors are located around the

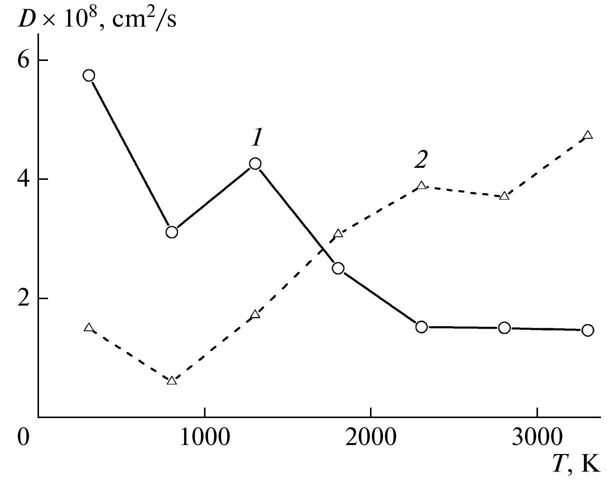

Fig. 3. The (*1*) *xy* and (*2*) *z* components of the self-diffusion coefficient of the elongated copper film on graphene whose atoms initially occupy nonadjacent cells in graphene.

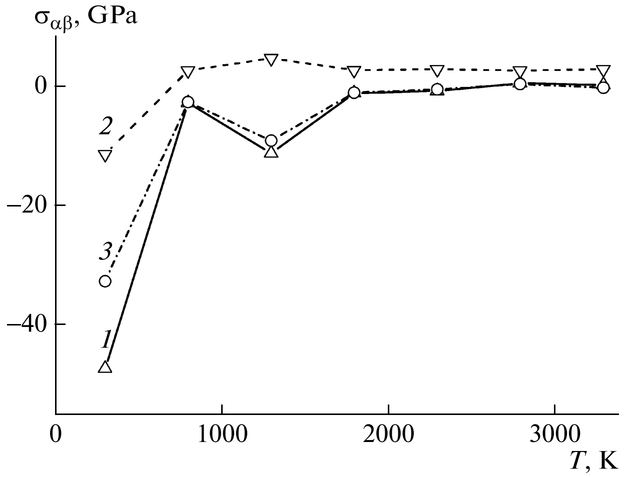

Fig. 4. Most significant stresses in the elongated copper film on graphene: (*1*) σ_{xx}, (*2*) σ_{yy}, and (*3*) σ_{xy}.

central atom at distances of up to ~1 nm. At distances $r > 1$ nm, the $g(r)$ functions for the films decay almost completely; i.e., there is no long-range ordering here. According to the shape of the $g(r)$ functions shown in Fig. 2, the model films differ in the medium-range order. The third film exhibits the highest stability against heating; even at 3300 K, ~2/3 of all of its Cu atoms remained in the film, forming a bound structure.

The kinetic and mechanical properties of the third Cu film formed with allowance for the graphene structure were studied in the form of the $D_{\leftrightarrow}$ and $D_{\updownarrow}$ components of the self-diffusion coefficient and nine components of the stress tensor $\sigma_{\alpha\beta}$. The horizontal component $D_{\leftrightarrow}$ (curve *1*) of the self-diffusion coefficient of Cu atoms tends to decrease as the temperature increases, while the vertical component $D_{\updownarrow}$ (curve *2*) tends to increase (Fig. 3). The decrease in the $D_{\leftrightarrow}$ values is caused by the gradual approach of Cu atoms, i.e., by the densification of the film because its initial packing density did not correspond to the stable state at given temperatures. The increase in $D_{\updownarrow}$ at elevated temperatures is explained by the increased mobility of atoms in a direction that is open for their motion. The increase in $D_{\leftrightarrow}$ at $T = 1300$ K may be interpreted as reaching the melting point in the Cu film because the melting temperature of bulk copper is 1357 K. The decrease in $D_{\updownarrow}$ at 800 and 2800 K may be regarded as fluctuations caused by the adjustment of the film structure to the graphene structure.

The film formed by Cu atoms arranged in a honeycomb structure experiences considerable stresses, the greatest of which at 300 K are σ_{xx}, σ_{xy}, and σ_{yy} (Fig. 4). These components of stress stay longer in the metal film as the stress temperature increases. As the temperature increases, all stresses dissipate. The interaction of Cu atoms with graphene affects the film structure; i.e., the film becomes structured in accordance with the crystal directions in graphene. If the stresses in the film are considered relative to the directions of the graphene sheet, then we can conclude that the long-living stresses are those in regions perpendicular to the zigzag and chair directions, including the zigzag–chair and chair–zigzag variants.

Thus the thermal stability of the monolayer copper film on graphene is considerably affected by the agreement between the arrangement of Cu atoms and the graphene structure. In addition, the stresses in the metal film are determined by the crystallographic directions of graphene.

ACKNOWLEDGMENTS

This study was financially supported by the Russian Foundation for Basic Research (project no. 13-08-00273).

REFERENCES

1. A. E. Galashev and V. A. Polukhin, Phys. Solid State **55**, 1733 (2013).
2. S. Wang, X. Huang, Y. He, et al., Carbon **50**, 2119 (2012).
3. A. Reina, X. T. Jia, J. Ho, et al., Nano Lett. **9**, 30 (2009).
4. K. S. Kim, Y. Zhao, H. Jang, et al., Nature **457**, 706 (2009).
5. G. Jo, M. Choe, C. Y. Cho, et al., Nanotecnology **21**, 175201 (2010).
6. T. Hayashi, S. Hirono, M. Tomita, and S. Umemura, Nature **381**, 772 (1996).

7. E. K. Athanassiou, R. N. Grass, and W. J. Stark, Nanotecnology **17**, 1668 (2006).
8. W. S. Seo, J. H. Lee, X. M. Sun, et al., Nature Mater. **5**, 971 (2006).
9. S. Stankovich, D. A. Dikin, G. H. B. Dommett, et al., Nature **442**, 282 (2006).
10. N. A. Luechinger, E. K. Athanassiou, and W. J. Stark, Nanotecnology **19**, 445201 (2008).
11. J. Lee, K. S. Novoselov, and H. S. Shin, ACS Nano **5**, 608 (2011).
12. J. Tersoff, Phys. Rev. B: Condens. Matter **37**, 6991 (1988).
13. J. Tersoff, Phys. Rev. B: Condens. Matter **39**, 5566 (1988).
14. S. J. Stuart, A. V. Tutein, and J. A. Harrison, J. Chem. Phys. **112**, 6472 (2000).
15. H. Rafii-Tabar, Phys. Rep. **325**, 239 (2000).
16. S. Jalili, C. Mochani, M. Akhavan, and J. Schofield, Mol. Phys. **110**, 267 (2012).
17. M. Moseler, F. Cervantes, S. Hofmann, et al., ACS Nano **4**, 7587 (2010).
18. Z. Xu and M. J. Buehler, J. Phys.: Condens. Matter **22**, 485301 (2010).
19. H. J. C. Berendsen, J. P. M. Postma, W. F. van Gunsteren, et al., J. Chem. Phys. **81**, 3684 (1984).
20. S. Yu. Davydov, Phys. Solid State **54**, 875 (2012).
21. P. M. Agrawal, B. M. Rice, and D. L. Thompson, Surf. Sci. **515**, 21 (2002).

Translated by L. Smolina